Electronic Supplementary Material (ESI) for ChemComm.
This journal is © The Royal Society of Chemistry 2017

Supporting Information

for

An Organoboron Compound with Wide Absorption Spectrum for Solar Cell Application

Fangbin Liu, Zicheng Ding, Jun Liu*, Lixiang Wang

State Key Laboratory of Polymer Physics and Chemistry

Changchun Institute of Applied Chemistry

Chinese Academy of Sciences, Changchun 130022, P. R. China

Email: liujun@ciac.ac.cn.

Contents

1. Materials and synthesis
2. OSCs device fabrication and measurement
3. TGA
4. DSC and XRD
5. DFT calculation results
6. AFM and TEM images
7. Charge mobility measurement
8. J_{sc} versus light intensity
9. J_{ph} versus effective voltage
10. Chemical structure of PTB7-Th
11. The absorption spectrum of blend film
12. References

1. Materials and synthesis

Materials. Commercially available solvents and reagents were used without further purification unless otherwise mentioned. Toluene and tetrahydrofuran were purified by distillation under Argon prior to use. PTB7-Th was purchased from 1-Material Chemscitech Inc. (Canada). 5,5'-dibromo-[2,2'-bipyridine]-3,3'-diamine, 5-(4,4,5,5-tetramethyl-1,3,2-dioxaborolan-2-yl)thiophene-2-carbaldehyde, and 2-(3-oxo-2,3-dihydro-1H-inden-1-ylidene)malononitrile were prepared according to the literature methods.[1,2]

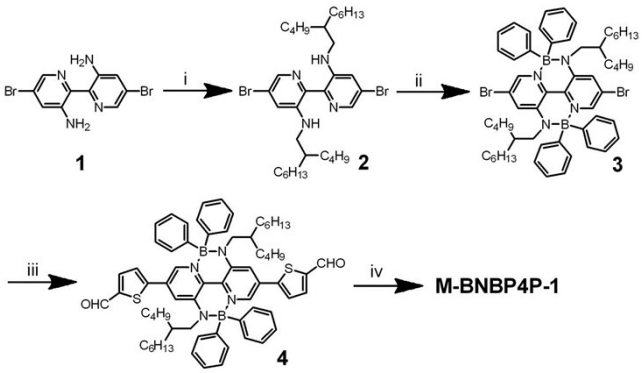

Scheme 1. Synthetic route of **M-BNBP4P-1**.

Synthesis of 5,5'-dibromo-N^3,$N^{3'}$-di-2-hexyldecyl-[2,2'-bipyridine]-3,3'-diamine (2): Under argon, to a solution of 5,5'-dibromo-2,2'-bipyridine-3,3'-diamine **(1)** (1.00 g, 2.92 mmol) in THF (45 mL) was added *n*-BuLi (2.4 M in hexane, 2.7 mL, 6.43 mmol) dropwise at −78 °C. After the mixture being stirred at −78 °C for 1 h, 1-iodine-2-butyloctane (1.90 g, 6.43 mmol) was added and the resulting mixture was stirred for 10 h at 75 °C. After removal of the solvents in reduced pressure, the residual was purified by silica gel column chromatography with CH_2Cl_2/hexane=1/5 as the solvent to give **2** as light yellow oil. Yield: 798 mg, 55%. ^{1}H NMR (400 MHz, C_6D_6, 25 °C): δ 10.24 (t, *J* = 3.6 Hz, 2H), 8.01 (d, *J* = 1.6 Hz, 2H), 7.08 (d, *J* = 1.6 Hz, 2H)，2.74 (m, *J* = 4.0 Hz, 4H), 1.57 (m, 2H), 1.43-1.17 (m, 32H), 0.97-0.87 (m, 12H). ^{13}C NMR (400 MHz, C_6D_6, 25 °C): δ 147.41, 138.20, 132.17, 120.37, 119.13, 46.08, 37.66, 32.91, 32.64, 32.27, 30.17, 29.43, 27.21, 23.49, 23.15, 14.42, 14.36. Anal. Calc. for $C_{34}H_{56}Br_2N_4$: C, 60.00; H, 8.29; Br, 23.48; N, 8.23. Found: C, 60.53; H, 8.01; Br, 23.22; N, 8.24

Synthesis of 3: A mixture of **2** (750 mg, 1.10 mmol), BPh_3 (1.330 g, 5.51 mmol) and toluene (30 mL) was stirred at 120 °C for 8 h. After removal of the solvents under reduced pressure, the residual was purified by silica gel column chromatography with CH_2Cl_2/hexane=1/5 as the eluent. The compound **3** was obtained as a red solid. Yield: 930 mg, 84%. ^{1}H NMR (400 MHz, C_6D_6, 25 °C): δ 7.83 (s, 2H), 7.53 (s, 2H), 7.25-7.10 (m, 20H), 3.24 (d, *J* = 5.8 Hz, 4H), 1.72 (m, *J* = 5.2 Hz, 2H), 1.36-0.97 (m, 32H), 0.96-0.76 (m, 12H). ^{13}C NMR (400 MHz, C_6D_6, 25 °C): δ 149.80, 134.65, 132.10, 131.03, 127.91, 127.05, 126.14, 121.23, 52.76, 36.21, 32.40, 32.19, 32.11, 30.03, 29.04, 26.88, 23.36, 23.06, 14.37, 14.24. Anal. Calc. for $C_{58}H_{74}B_2Br_2N_4$: C, 69.06; H, 7.39; B, 2.14; Br, 15.84; N, 5.55. Found: C, 68.81; H, 7.67; B, 2.33; Br, 15.53; N, 5.66

Synthesis of 4: A mixture of **3** (441 mg, 0.437 mmol), 5-(4,4,5,5-tetramethyl-1,3,2-dioxaborolan-2-yl)thiophene-2-carbaldehyde (261 mg, 1.093 mmol), $Pd(PPh_3)_4$ (51 mg, 0.044 mmol), THF (30 ml), aqueous K_2CO_3 (2M, 0.66 mL, 1.311mmol) was stirred under argon at 75 °C overnight. After cooled to room temperature, the reaction mixture was extracted with CH_2Cl_2. The organic phase was washed with water, dried over anhydrous Na_2SO_4, filtered and concentrated. The residual was purified by silica gel column chromatography with CH_2Cl_2/hexane=1/2 as the eluent to afford **4** as blue solid. Yield: 388 mg, 82%. ^{1}H NMR (400 MHz, C_6D_6, 25 °C): δ 9.30 (s, 2H), 8.02 (d, *J* = 1.2 Hz, 2H)， 7.68 (d, *J* = 1.2 Hz, 2H), 7.50-7.25 (m, 20H), 6.63 (d, *J* = 3.2 Hz, 2H), 6.51 (d, *J* = 3.2 Hz, 2H), 3.50 (d, *J* = 2.4 Hz, 4H), 1.89 (m, 2H), 1.52-1.00 (m, 32H), 0.99-0.70 (m, 12H). ^{13}C NMR (400 MHz, C_6D_6, 25 °C): δ 181.85, 149.50, 144.81, 136.59, 135.08, 131.94, 130.57, 129.33, 127.31, 125.85, 120.36, 53.17, 36.71, 33.02, 32.69, 32.47, 30.42, 29.66, 27.53, 27.45, 23.75, 23.32, 14.62, 14.56. Anal. Calc. for $C_{68}H_{80}B_2N_4O_2S_2$: C, 76.25; H, 7.53; B, 2.02; N, 5.23; O, 2.99; S, 5.99. Found: C, 75.96; H, 7.83; B, 2.22; N, 5.20; O, 3.43; S, 5.36。

Synthesis of M-BNBP4P-1: A mixture of **4** (150 mg, 0.140 mmol), 2-(3-oxo-2,3-dihydroinden-1-ylidene)malononitrile (82 mg, 0.420 mmol), pyridine (0.5 mL) and toluene (15 mL) was stirred at 75 °C for 6 h. After cooled to room temperature, the mixture was poured into methanol (100 mL) and filtered. The solid was purified by silica gel column chromatography with CH_2Cl_2/hexane=2/1 as the eluent. Yield: 169

mg, 85%. ^{1}H NMR (400 MHz, C_6D_6, 25 °C)：δ 8.43-8.40 (m, 4H), 8.15 (d, *J* = 1.2 Hz, 2H), 7.97 (d, *J* = 1.2 Hz, 2H)，7.58 (m, 2H), 7.43 (s, 8H), 7.26 (m, 12H), 6.96 (t, *J* = 2.8 Hz, 2H), 6.86 (m, 4H), 6.60 (d, *J* = 3.2 Hz, 2H), 3.64 (d, *J* = 5.2 Hz, 4H), 2.08 (m, *J* = 5.2 Hz and 4.4 Hz, 2H), 1.57-1.15 (m, 32H), 1.05-0.81 (m, 12H). ^{13}C NMR (400 MHz, C_6D_6, 25 °C)：δ 187.81, 159.35, 152.80, 149.63, 145.24, 140.44, 138.20, 137.30, 136.69, 135.16, 134.33, 132.07, 130.74, 129.80, 128.54, 128.45, 128.35, 128.25, 128.16, 128.06, 127.36, 126.36, 125.51, 125.00, 123.76, 120.20, 114.84, 114.59, 72.19, 53.39, 36.89, 33.17, 32.84, 32.46, 30.51, 29.69, 27.49, 23.85, 23.39, 14.61, 14.59. Anal. Calc. for $C_{86}H_{88}B_2N_4O_4S_2$: C, 77.82; H, 6.68; B, 1.63; N, 4.22; O, 4.82; S, 4.83. Found: C, 77.12; H, 6.77; B, 1.98; N, 4.56; O, 4.32; S, 5.25.

Characterization. ^{1}H and ^{13}C NMR spectra were measured with a Bruker AV-400 (400 MHz for ^{1}H NMR and ^{13}C NMR) spectrometer with C_6D_6 as the solvent and TMS as an internal standard. Elemental analyses were carried out using a VarioEL elemental analyzer. UV-vis absorption spectra were measured with a Shimadzu UV-3600 spectrometer. Thermogravimetric analysis (TGA) measurement was performed using a Perkin-Elmer 7 instrument under nitrogen flow at a heating rate of 10 °C min^{-1}. Differential scanning calorimetry (DSC) was performed at the heating/cooling rate of 10 °C min^{-1} with a TA Instruments Q2000. X-ray diffraction (XRD) measurement was performed using a Bruker D8 Discover reflector, and the sample was prepared by dropcasting with chlorobenzene solution (10 mg mL^{-1}) on silicon substrate. Atomic force microscopy (AFM) was recorded with a SPA300HV (Seiko Instruments, Inc., Japan) in tapping mode. Cyclic voltammetry (CV) was performed using an CHI660a electrochemical workstation with a standard three-electrode system consisting of a cylindrical platinum working electrode, platinum mesh counter electrode and Ag/Ag^{+} reference electrode. CV measurements were carried out with the solution in anhydrous and deoxygenated dichloromethane with the concentration of 0.3 mM containing *n*-Bu_4NClO_4 (0.1 M) as the electrolyte at a scan rate of 100 mV s^{-1}. Ferrocene (Fc) was used as the standard. LUMO and HOMO energy levels were calculated from the equations: $E_{LUMO} = -(E_{red} + 4.8)$ eV and $E_{HOMO} = -(E_{ox} + 4.8)$ eV, where E_{red} and E_{ox} are the onset potentials vs. Fc/Fc^{+} of the reduction and oxidation processes,

respectively.

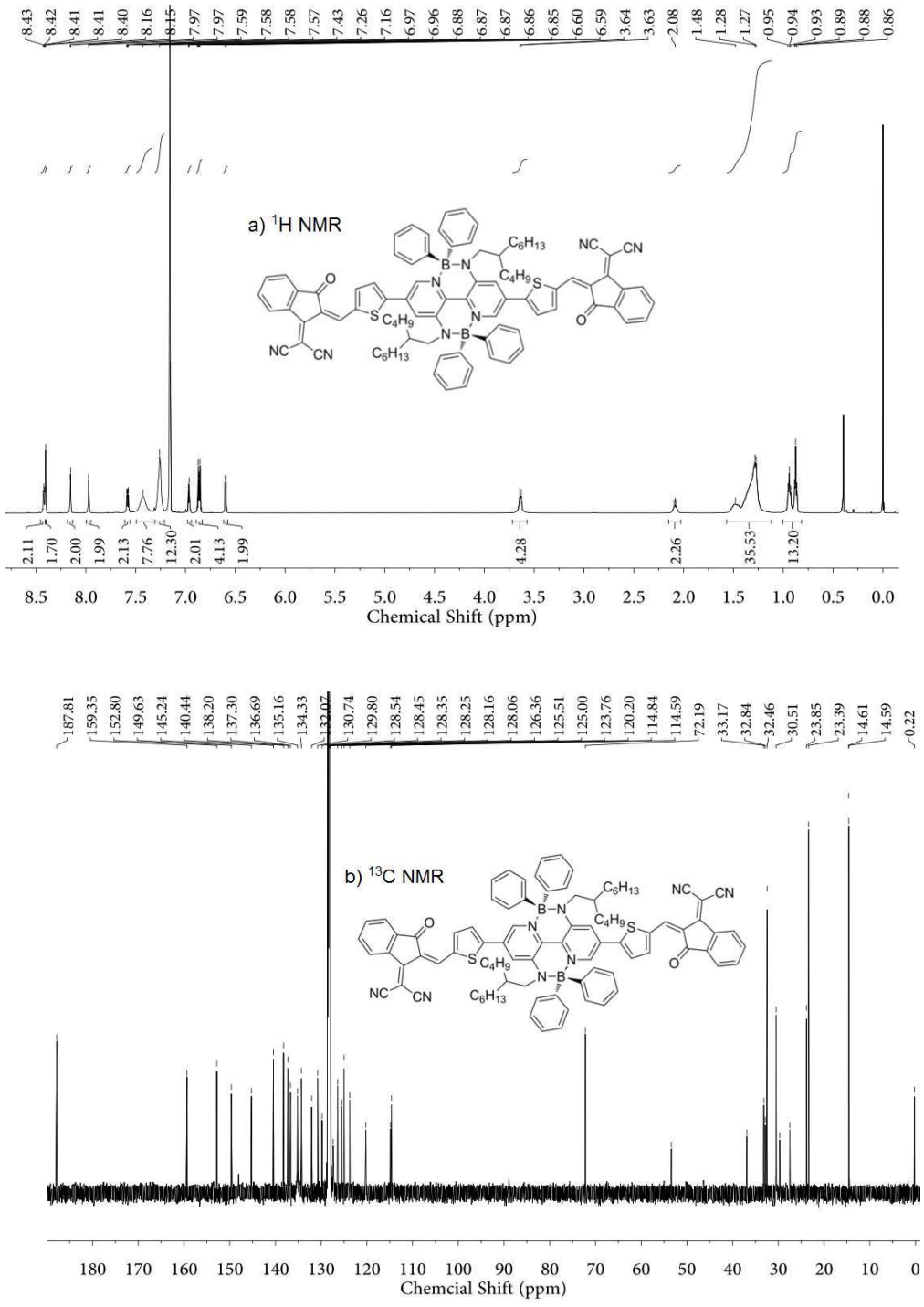

Figure S1. a) ^{1}H NMR and b) ^{13}C NMR spectra of **M-BNBP4P-1**.

2. OSCs device fabrication and measurement

OSC device was fabricated with an architecture of indium tin oxide (ITO)/ poly(3,4-ethylenedioxythiophene) doped with polystyrene sulfonate (PEDOT:PSS)/PTB7-Th:**M-BNBP4P-1**/Ca/Al. Patterned ITO glass substrates were cleaned by sequential ultrasonication in detergent, deionized water, acetone, and isopropyl alcohol, followed by heating at 120 °C for 30 min and UV-ozone treatment for 30 min. PEDOT:PSS (Clevios PVP Al4083 from H. C. Starck Inc.) with the thickness of 40 nm was spin-coated on the ITO substrates and annealed at 120 ^{o}C for 30 min. The active layer was spin-coated from the solution of PTB7-Th and **M-BNBP4P-1** in chlorobenzene (20 mg mL^{-1}) at 2000 rpm, which resulted in the active layer thickness of 110 nm. Then the active layer was heated at 100 °C for 10 minutes. Finally, the device was transferred to a vacuum chamber and Ca (20 nm)/Al (100 nm) was sequentially deposited by thermal evaporation at the pressure of about 2×10^{-4} Pa. The active area of each device was 8.0 mm^2.

The current density (*J-V*) curves of the OSC devices were measured using a computer-controlled Keithley 2400 source meter under 100 mW cm^{-2} AM 1.5G simulated solar light illumination provided by a XES-40S2-CE Class Solar Simulator (Japan, SAN-EI Electric Co., Ltd.). The EQE was measured using a Solar Cell Spectral Response Measurement System QE-R3011 (Enlitech Co., Ltd.), which was calibrated with a crystal silicon photovoltaic cell before use.

3. TGA

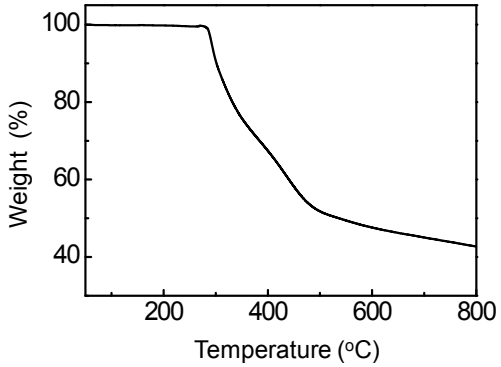

Figure S2. TGA plot of **M-BNBP4P-1**. In N_2 atmosphere, **M-BNBP4P-1** has good thermal stability with decomposition temperature (T_d) at 5% weight loss of 288 °C.

4. DSC and XRD

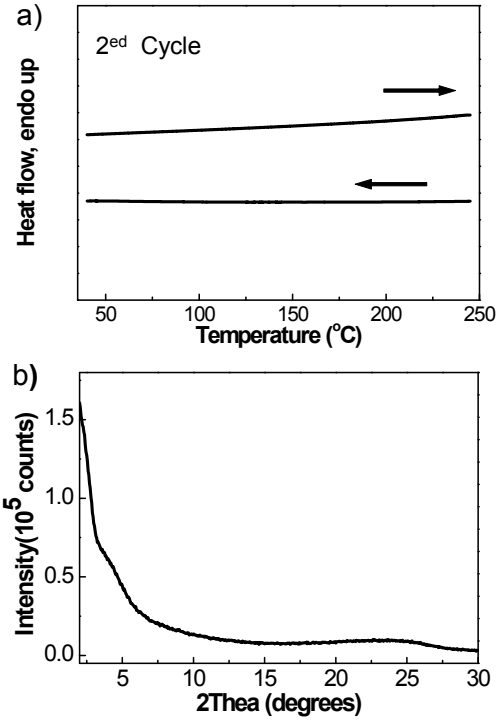

Figure S3. a) DSC curves and b) XRD pattern of **M-BNBP4P-1**. The second cycle of DSC measurement is shown.

5. DFT calculation results

All calculations were carried out using Gaussian 09. The geometry structure of **M-BNBP4P-1** were optimized by using DFT calculations (B3LYP/6-31G*) and the alkyl chains have been replaced by methyl for clarity. Time-dependent DFT (TD-DFT) calculations were performed at the B3LYP/6-31G* level of theory to more precisely elucidate the absorption of **M-BNBP4P-1**. TD-DFT calculation for the $S_0 \rightarrow S_n$ transitions using the same functional and basis set were then performed based on the optimized structure at ground state.

Excitation energies and oscillator strengths (Oscillator strength exceeding 0.1):

Excited State 1: Energy: 1.4610 eV Wavelength: **848.6 nm** Oscillator strength: **0.5406** Configulations: **HOMO→LUMO (0.70516);**

Excited State 6: Energy: 2.3050 eV Wavelength: **537.9 nm** Oscillator strength: **0.2454** Configulations: **HOMO→LUMO+1 (0.69991);**

Excited State 7: Energy: 2.4336 eV Wavelength: **509.5 nm** Oscillator strength: **0.8902** Configulations: **HOMO-4→LUMO (0.16303); HOMO-2→LUMO (0.57666); HOMO→ LUMO+4 (-0.34843);**

Excited State 10: Energy: 2.5472 eV Wavelength: **486.8 nm** Oscillator strength: **0.4766** Configulations: **HOMO-8→LUMO (0.15556); HOMO-6→LUMO (-0.11425); HOMO-4→LUMO (0.56391); HOMO-2→LUMO (-0.28798); HOMO→ LUMO+4 (-0.22390);**

Excited State 14: Energy: 2.6496 eV Wavelength: 467.9 nm Oscillator strength: 0.1388 Configulations: HOMO-8→LUMO (0.67600); HOMO-4→LUMO (-0.10907);

Excited State 27: Energy: 3.0073 eV Wavelength: 412.3 nm Oscillator strength: 0.1695 Configulations: HOMO-12→LUMO (0.13025); HOMO-9→LUMO+1 (0.51556); HOMO-7→LUMO+1 (-0.23619); HOMO-5→LUMO+1 (0.12836); HOMO-2→LUMO+2 (0.24602); HOMO-1→LUMO+2 (0.13538).

The transition energies and oscillator strengths simulated by the TD-DFT (B3LYP/6-31G*) calculations resulted in two absorption bands for **M-BNBP4P-1**. The calculation results agree well with the measured absorption spectrum (Figure S4), and explain the relation between the molecule structure and absorption spectra. The electronic transition HOMO→LUMO (Excited State 1) corresponding to the energy of 1.4610 eV (wavelength at 848.6 nm) results in the low-energy absorption band in the absorption spectrum. The high-energy absorption band around 500 nm is attributed to six types of electronic transitions, HOMO-8→LUMO, HOMO-6→LUMO, HOMO-4→LUMO, HOMO-2→LUMO, HOMO→LUMO+1 and HOMO→LUMO+4 (illustrated by Excited State 6, 7 and 10). The main orbital configurations and electronic transitions of **M-BNBP4P-1** mentioned above were shown in Figure S5.

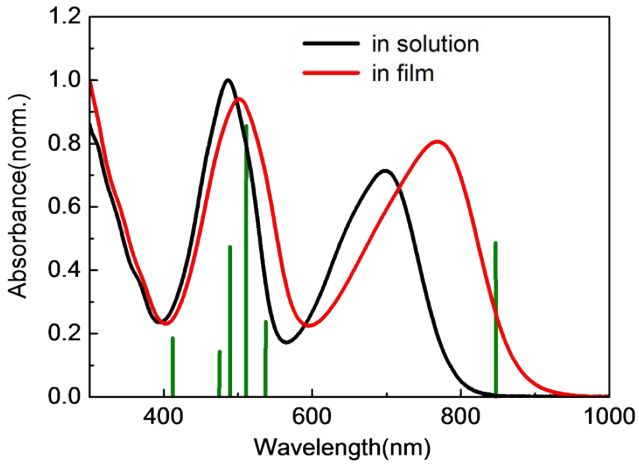

Figure S4. UV/Vis absorption spectra of **M-BNBP4P-1** in chlorobenzene solution and in thin film. The green bar shows the transition energies and oscillator strengths simulated by the TD-DFT (B3LYP/6-31G*) calculations.

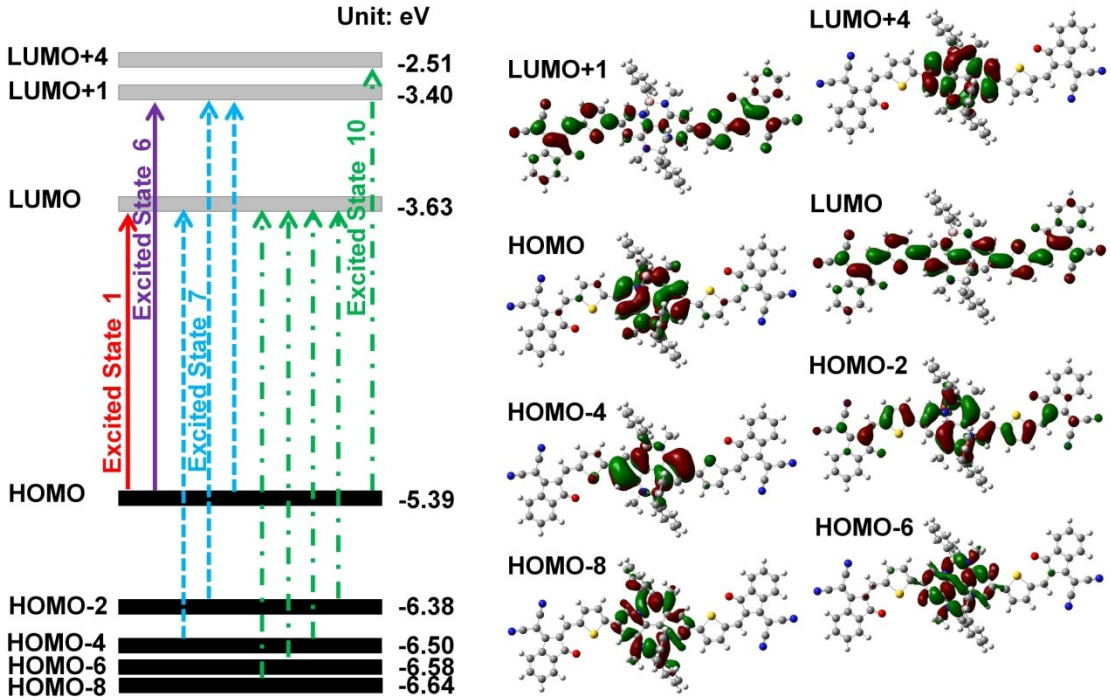

Figure S5. Schematic diagrams showing the main orbital configurations and electronic transitions of **M-BNBP4P-1** based on the TD-DFT (B3LYP/6-31G*) calculation.

6. AFM images

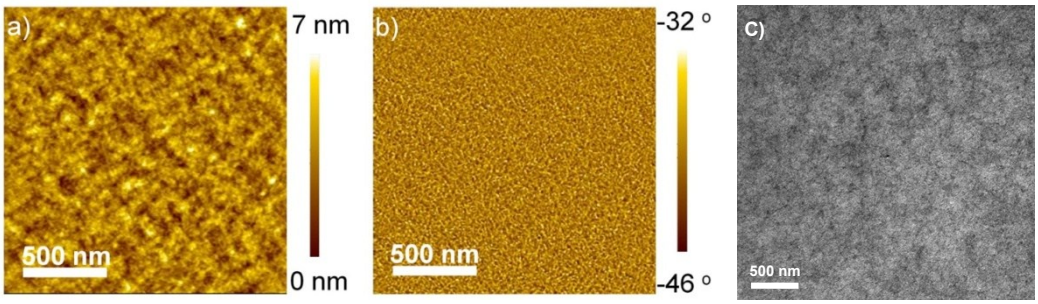

Figure S6. a) AFM height image, b) phase image and c) TEM image of the PTB7-Th:M-BNBP4P-1 blend film.

7. Charge mobility measurement

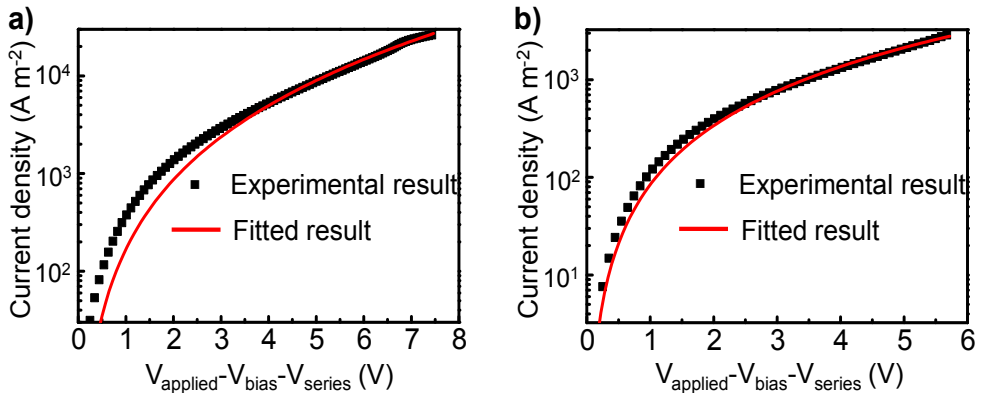

Figure S7. J-V curves and SCLC fitting of a) the hole-only device and b) electron-only device of the PTB7-Th:**M-BNBP4P-1** blend film.

Charge carrier mobilities of the PTB7-Th:**M-BNBP4P-1** blend were measured based on the SCLC method with the hole-only device (ITO/PEDOT:PSS/active layer/Al) and electron-only device (ITO/PEIE/active layer/Ca/Al). The *J-V* curves were fitted to a space-charge-limited function:

$$J = \frac{9\varepsilon_0\varepsilon_r\mu_0 V^2}{8L^3}\exp\left(0.89\beta\sqrt{\frac{V}{L}}\right) \quad (1)$$

where J is the current density, L is the film thickness of the active layer, μ_0 is the charge mobility, ε_r is the relative dielectric constant of the transport medium, ε_0 is the permittivity of free space, V (V_{appl} - V_{bi}) is the internal voltage in the device, where V_{appl}

is the applied voltage to the device and V_{bi} is the built-in voltage due to the relative work function difference of the two electrodes. The hole and electron mobilities are estimated to be 6.87×10^{-4} cm^2 V^{-1} s^{-1} and 1.47×10^{-4} cm^2 V^{-1} s^{-1}, respectively. The high and balanced hole/electron mobilities of the blend are in agreement with the high OSCs performance.

8. J_{sc} versus light intensity

The dependence of short-circuit current on the light intensity was measured to study charge recombination in the OSC devices. As reported, the J_{sc} follows a power-law dependence on the illumination intensity ($J_{sc} \propto P_{light}^{\alpha}$, where P_{light} is light intensity and α is the calculated power-law exponent). If all free carriers are swept out and collected at the electrodes prior to recombination, α should be equal to 1. In this work, the current density shows a linear dependence on the light intensity in logarithmic coordinates with a slope (α) of 0.98, indicating efficient sweep-out of carriers and well suppressed bimolecular recombination.

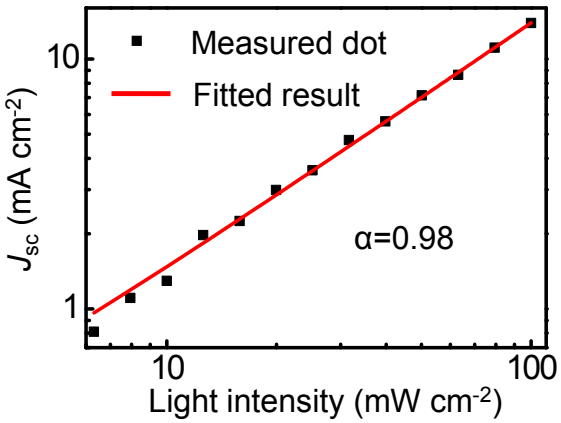

Figure S8. J_{sc} versus light intensity characteristic of the OSC device based on PTB7-Th:**M-BNBP4P-1** blend.

9. J_{ph} versus effective voltage

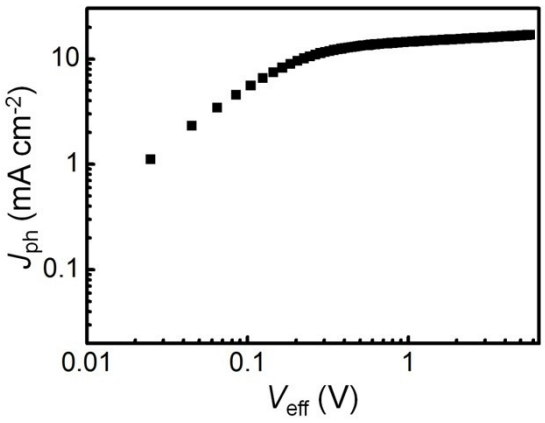

Figure S9. Photocurrent density (J_{ph}) versus effective voltage (V_{eff}) characteristic of the OSCs device based on PTB7-Th:**M-BNBP4P-1** blend.

The photocurrent density (J_{ph}) versus the effective voltage (V_{eff}) was measured to study the charge generation and extraction properties. J_{ph} can be defined as $J_{ph} = J_L - J_D$, where J_L and J_D are the photocurrent densities under illumination and in the dark, respectively. V_{eff} can be defined as $V_{eff} = V_{oc} - V_{bias}$, where V_{oc} is the voltage at which the photocurrent is zero and V_{bias} is the applied voltage. Therefore, V_{eff} determines the electric field in the bulk region and thereby affects the carrier transport and the photocurrent extraction. The plot of J_{ph} versus V_{eff} is presented in Figure S7. At high V_{eff} values, mobile charge carriers rapidly move toward the corresponding electrodes with minimal recombination. J_{ph} reaches saturation (15.58 mA cm^{-2}) at $V_{eff} \geqslant 2.5$ V, suggesting that all photogenerated excitons are dissociated into free charge carriers and charge carriers are collected at the electrodes very efficiently. Under short-circuit condition, J_{ph} is 14.62 mA cm^{-2}, which is ~94% of all photogenerated carriers collected by the electrodes, indicating efficient photogenerated exciton dissociation and charge collection for PTB7-Th:**M-BNBP4P-1** device.

10. Chemical structure of PTB7-Th

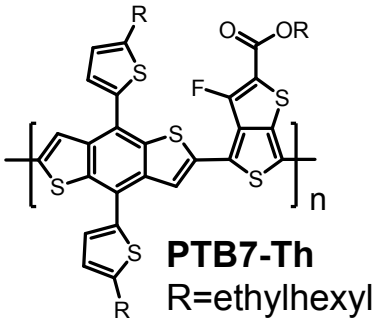

11. The absorption spectrum of blend film

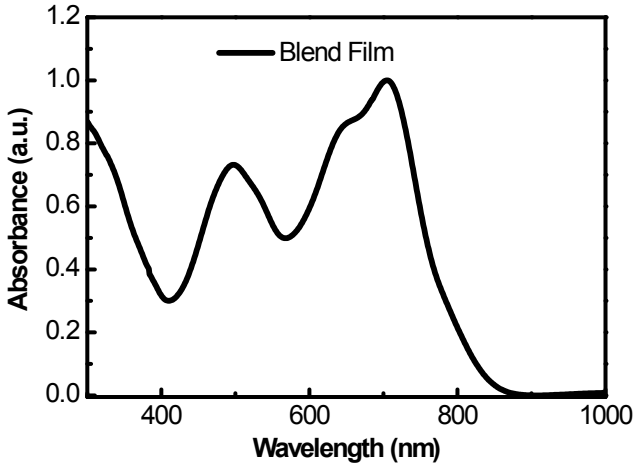

Figure S10. The absorption spectrum of PTB7-Th:**M-BNBP4P-1** blend film.

12. References

1. C. Dou, X. Long, Z. Ding, Z. Xie, J. Liu, L. Wang, An Electron-Deficient Building Block Based on the B-N Unit: An Electron Acceptor for All-Polymer Solar Cells. *Angewandte Chemie International Edition.* **2016***, 55,* 1436-1440; *Angewandte Chemie*, **2016**, *128*, 1458-1462.
2. Q. Zhang, B. Kan, F. Liu, G. Long, X. Wan, X. Chen, Y. Zuo, W. Ni, H. Zhang, M. Li, Z. Hu, F. Huang, Y. Cao, Z. Liang, M. Zhang, T.-P. Russell, Y. Chen, Small-molecule Solar Cells with Efficiency over 9%. *Nature Photonics*, **2014**, *9*, 35-41.